



Title	Transient dynamics of molecular devices under a steplike pulse bias
Author(s)	Wang, B; Xing, Y; Zhang, L; Wang, J
Citation	Physical Review B (Condensed Matter and Materials Physics), 2010, v. 81 n. 12 article no. 121103(R)
Issued Date	2010
URL	http://hdl.handle.net/10722/123836
Rights	Physical Review B (Condensed Matter and Materials Physics). Copyright © American Physical Society.

Transient dynamics of molecular devices under a steplike pulse bias

Bin Wang, Yanxia Xing, Lei Zhang, and Jian Wang*

Department of Physics and the Center of Theoretical and Computational Physics, The University of Hong Kong, Pokfulam Road, Hong Kong, China

(Received 19 January 2010; published 17 March 2010)

We report first-principles investigation of time-dependent current of molecular devices under a steplike pulse. Our results show that although the switch-on time of the molecular device is comparable to the transit time, much longer time is needed to reach the steady state. In reaching the steady state the current is dominated by resonant states below Fermi level. The contribution of each resonant state to the current shows the damped oscillatory behavior with frequency approximately equal to half of the bias of steplike pulse and decay rate determined by the life time of the corresponding resonant state. We found that all the resonant states below Fermi level have to be included for accurate results. This indicates that going beyond wideband limit is essential for a quantitative analysis of transient dynamics of molecular devices.

DOI: [10.1103/PhysRevB.81.121103](https://doi.org/10.1103/PhysRevB.81.121103)

PACS number(s): 73.63.-b, 72.30.+q, 71.15.Mb

Anticipating a variety of technological applications, molecular scale conductors and devices are the subject of increasingly more research in recently years. One of the most important issues of molecular electronics concerns the dynamic response of molecular devices to external parameters.¹⁻⁹ For ac quantum transport in such small devices, atomic details and nonequilibrium physics must be taken into account. So, in principle, one should use the theory of nonequilibrium Green's function (NEGF) (Ref. 10) coupled with the time-dependent density-functional theory (TDDFT) (Ref. 11) to study the time-dependent transport of molecular devices. Practically, it is very difficult to implement it at present stage due to the huge computational cost. One possible way to overcome this problem is to use the adiabatic approximation, an approach widely used in mesoscopic physics. In this approach, one starts from a steady-state Hamiltonian and adds the time-dependent electric field adiabatically. This is a reasonable approximation since most of the time the applied electric field is much smaller than the electrostatic field inside the scattering region. In addition, it has been shown numerically⁷ that dc transport properties such as I-V curve obtained from the equation of motion method coupled with TDDFT agrees with that obtained by the method of NEGF coupled with the DFT.^{12,13} Hence, under the adiabatic approximation, one could replace TDDFT by DFT and use the NEGF+DFT scheme to calculate ac transport properties of molecular devices.

We consider a system that consists of a scattering region coupled to two leads with the external time-dependent pulse bias potential $v_\alpha(t)$. The time-dependent current for a step-like pulse has been derived exactly going beyond the wide-band limit by Maciejko *et al.*⁵ Since the general expression for the current involves triple integrations, it is extremely difficult if not impossible to calculate the time-dependent current for real systems such as molecular devices. In this regard, approximation has to be made in order to carry out time-dependent simulations of molecular devices. We note that the simplest approximation is the so-called wide-band approximation where self-energies $\Sigma^{r,a}$ are assumed to be constants independent of energy.¹⁴ However, there are two problems when applying this approximation to investigate the dynamics of molecular devices. First of all, one assumes

implicitly that the contribution to the transient current is dominated by only one resonant level with a constant line-width function Γ in the system in such an approximation. As we shall show below that this is not a good assumption in first-principles investigation of the dynamics of molecular devices because there could be several resonant levels that significantly contribute to the transient current in molecular devices. Second, the wide-band limit cannot reproduce the correct dc I-V curve obtained from first principles. For instance, the current driven by an upward pulse approaches to a steady-state current I at $t \rightarrow \infty$. By assuming the wide-band limit one can get a very different current that depends on the choice of Γ . In this Rapid Communication, we propose an approximate formula of transient current that is suitable for numerical calculation for real molecular devices. Our scheme is an approximation of the exact solution of Maciejko *et al.*⁵ while keeping essential physics of dynamic systems. Using this scheme, we have calculated the transient current for several molecular devices. We found that all the resonant states below Fermi level contribute to the transient current. Each resonant state gives a damped oscillatory behavior with frequency approximately equal to half of the bias of pulse and decay rate equal to its life time. Because of sharp resonances, it takes much longer time for the current to relax to the equilibrium value. For instance, for a CNT-DTB-CNT structure with transit time $L/v_F=1$ fs, the relaxation time can reach several ps due to the resonant state with long lifetime. Our results indicated that going beyond wide-band limit is crucial for accurate predictions of dynamic response of molecular devices.

From Refs. 5 and 14, the current is expressed as ($\hbar=1$),

$$J_\alpha(t) = 2 \operatorname{Re} \int \frac{d\epsilon}{2\pi} \operatorname{Tr}[J_\alpha(\epsilon)] \quad (1)$$

where

$$J_\alpha(\epsilon) = A_\alpha(t, \epsilon) \Sigma_\alpha^{<,0}(\epsilon) + \sum_\beta A_\beta(t, \epsilon) \Sigma_\beta^{<,0}(\epsilon) F_{\beta\alpha}(t, \epsilon) \quad (2)$$

where $\Sigma^{<,0}$ and $\Sigma^{a,0}$ are equilibrium self-energies and $A_\alpha(t, \epsilon)$ and $F_{\beta\alpha}(t, \epsilon)$ have different definitions for upward

and downward pulses (see Ref. 5 for details). In the absence of ac bias, $A_\alpha(t, \epsilon)$ is just the Fourier transform of retarded Green's function. As discussed in Ref. 10 that the first term in Eq. (2) corresponds to the current flowing into the central scattering region from lead α while the second term corresponds to the current flowing out from the central region into lead α . From Eq. (1) we see that in order to calculate the transient current for a pulse bias we need to include the states with energy from $-\infty$ to the Fermi energy. This is very different from dc case where only the states with energy in the range $v_L - v_R$ about Fermi level contribute. Physically, this can be understood as follows. For ac transport with a sinusoidal bias $\cos(\omega t)$, the photon assisted tunneling is significant only for the first a few sidebands.¹⁰ The steplike pulse can be expanded in terms of sinusoidal bias with continuous distribution of frequencies and each sinusoidal bias generates a photon sideband that facilitates the photon assisted tunneling. Hence we expect that all the resonant states below Fermi level should be included and carefully examined in the calculation of transient current. Note that Eqs. (1) and (2) are exact expressions with $A_\alpha(t, \epsilon)$ and $F_{\beta\alpha}(t, \epsilon)$ given in Ref. 5. Our approximation is made on $A_\alpha(t, \epsilon)$ and $F_{\beta\alpha}(t, \epsilon)$. For the upward pulse, $A_\alpha(t, \epsilon)$ and $F_{\beta\alpha}(t, \epsilon)$ are given by the following ansatz:

$$A_\alpha^u(t, \epsilon) = A_{1\alpha}^u(t, \epsilon) + A_{2\alpha}^u(t, \epsilon) \quad (3)$$

with

$$A_{1\alpha}^u(t, \epsilon) = \int \frac{dE}{2\pi i} \frac{e^{i(\epsilon - E + qv_\alpha)t}}{E - \epsilon - i0^+} \bar{G}_0^r(E, \epsilon)$$

$$A_{2\alpha}^u(t, \epsilon) = \int \frac{dE}{2\pi i} \frac{1 - e^{i(\epsilon - E + qv_\alpha)t}}{E - \epsilon - qv_\alpha - i0^+} \bar{G}_\alpha^r(E, \epsilon) \quad (4)$$

and

$$[F_{\alpha\beta}^u(t, \epsilon)]^\dagger = \sum_\beta^{r,0}(\epsilon) A_{1\alpha}^u + \sum_\beta^{r,0}(\epsilon - qv_\beta + qv_\alpha) A_{2\alpha}^u \quad (5)$$

where

$$\bar{G}_0^r(E, \epsilon) = 1/[E - H - U_{eq} - \sum^{r,0}(\epsilon)] \quad (6)$$

and

$$\bar{G}_\alpha^r(E, \epsilon) = 1/\left[E - H - U - \sum_\beta^{r,0}(\epsilon + qv_\alpha - qv_\beta)\right] \quad (7)$$

with $q = -e$; U_{eq} and U are, respectively, the equilibrium Coulomb potential and dc Coulomb potential at bias $v_L - v_R$. As will be illustrated in the examples given below this ansatz can be easily implemented to calculate the transient current for real molecular devices. Importantly, the results obtained from the ansatz captured essential physics of molecular devices. We wish to emphasize that our ansatz goes beyond the wide-band limit. It agrees with the expression of time-dependent current obtained by Wingreen *et al.* in the wide-band limit¹⁴ and produces correct dc current at $t=0$ and $t \rightarrow \infty$. We have applied our method to the exact solvable model discussed in Ref. 5. Our result is in good agreement with that in Ref. 5.

Note that $\bar{G}_0^r(E, \epsilon)$ and $\bar{G}_\alpha^r(E, \epsilon)$ are different from the

usual definition of Green's functions, they allow us to perform contour integration over energy E in Eqs. (4) and (5) by closing a contour with an infinite radius semicircle at lower half plane. For a constant ϵ , we have the following eigenequations:

$$(H + U_{eq} + \sum^{r,0}(\epsilon))|\psi_n^0\rangle = \epsilon_n^0|\psi_n^0\rangle$$

$$(H + U_{eq} + \sum^{a,0}(\epsilon))|\varphi_n^0\rangle = \epsilon_n^{0*}|\varphi_n^0\rangle. \quad (8)$$

Expanding $\bar{G}_0^r(E, \epsilon)$ in terms of its eigenfunctions $|\psi_n^0\rangle$ and $|\varphi_n^0\rangle$, we have¹⁵

$$\bar{G}_0^r(E, \epsilon) = \sum_n |\psi_n^0\rangle\langle\varphi_n^0|/(E - \epsilon_n^0 + i0^+). \quad (9)$$

With similar expression for $\bar{G}_\alpha^r(E, \epsilon)$, Eq. (4) can be written as¹⁶

$$A_{1\alpha}^u = \sum_n \frac{e^{i(\epsilon - \epsilon_n^0 + qv_\alpha)t}}{\epsilon - \epsilon_n^0 + i0^+} |\psi_n^0\rangle\langle\varphi_n^0|$$

$$A_{2\alpha}^u = \sum_n \frac{1 - e^{i(\epsilon - \epsilon_n + qv_\alpha)t}}{\epsilon - \epsilon_n + qv_\alpha + i0^+} |\psi_n\rangle\langle\varphi_n|. \quad (10)$$

Now we show that our formalism gives the correct limits. At $t=0$ we have $A_\alpha^u(t, \epsilon) = G_0^r(\epsilon)$ and $F_{\beta\alpha}^u(t, \epsilon) = G_0^a(\epsilon) \sum_\alpha^{a,0}(\epsilon)$ with $G_0^r(\epsilon)$ the equilibrium Green's function. This shows that the current from Eq. (2) is zero. Since all the poles ϵ_n^0 and ϵ_n in Eq. (10) are on the lower half plane, at $t \rightarrow \infty$ we have $A_\alpha^u = G^r(\epsilon + qv_\alpha)$ and $F_{\beta\alpha}^u = G^a(\epsilon + qv_\beta) \sum_\alpha^{a,0}(\epsilon + qv_\beta - qv_\alpha)$ where $G^r(\epsilon)$ is the Green's function with dc bias v_α at $t \rightarrow \infty$. Substituting expressions of A_α^u and $F_{\beta\alpha}^u$ into Eq. (1), it gives the same dc current at the bias $v_L - v_R$. So far, we have discussed the ac conduction current $J_\alpha(t)$ under pulselike bias. The displacement current J_α^d due to the charge pileup dQ/dt inside the scattering region can be included using the method of current partition:^{17,18} $J_\alpha^d = -(J_L + J_R)/2$ so that the total current is given by $I_L = (J_L - J_R)/2$.¹⁰

With the formalism established, we now proceed to calculate the dynamic response of molecular devices. We have used the first-principles quantum transport package MATDICAL.¹² To calculate the transient current for steplike pulse, we need to go through the following steps: (1) calculate two potential landscapes using NEGF-DFT package: the equilibrium potential U_{eq} at $t=0$ and the dc potential U at $t = \infty$. (2) With U_{eq} and U obtained, one solves eigenvalue problem using Eq. (8) and its counterpart for U , then find $A_{1\alpha}^u$ and $A_{2\alpha}^u$ from Eq. (10), and finally A_α^u and $F_{\beta\alpha}^u$ can be calculated from Eqs. (3) and (5).

Inset of Fig. 1(a) shows the structure of Al-C₄-Al where Al leads are along (100) direction. The nearest distance between Al leads and the carbon chain is 3.781 a.u. and the distance of C-C bond is 2.5 a.u. (1 a.u. = 0.529 Å). In our calculation, one unit cell of Al lead consists of 9 Al atoms and total 40 atoms were included in the simulation box. Figure 1 shows the total transient currents $I_L(t)$ of the Al-C₄-Al structure with various voltages $v_L(t) = -v_R(t)$. Following observations are in order. First of all, for all bias voltages the transient currents reached the correct limits at $t=0$ and $t=\infty$.

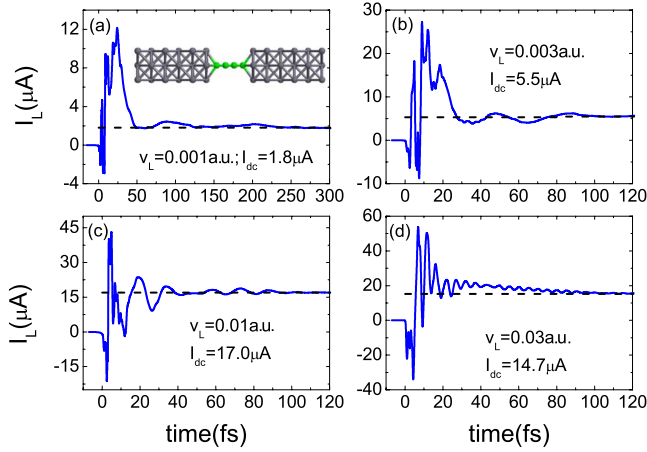


FIG. 1. (Color online) Transient current of Al-C₄-Al structure at different bias $v_L=0.001, 0.003, 0.01, 0.03$ a.u. The solid line shows the transient current and the dashed line is the dc current I_{dc} at bias $v_L-v_R=2v_L$. Inset of Fig. 1(a): schematic plot of the Al-C₄-Al structure.

Second, we see that once steplike voltage is turned on in the lead, currents oscillate rapidly with large amplitude in the first a few fs and then gradually approach to the steady-state values (I_{dc} shown in the figure).¹⁹ In the first 10–30 fs, the current is much larger than that of the steady-state value which agrees with the results obtained using first-principles calculation with wide-band limit.⁷ For the Al-C₄-Al structure, the relaxation time (time to reach to steady state) is roughly 120 fs and the switch-on time (the time to reach the maximum current) is about 5–10 fs. For Al leads, the Fermi velocity is about 2×10^6 m/s which corresponds to a transit time of 1.3 fs for the Al-C₄-Al structure whose size is about $L=47$ a.u.. Third, we observe that the dc limit I_{dc} at $v_L=0.01$ a.u. is larger than that at $v_L=0.03$ a.u.. This is due to the appearance of the negative differential resistance at about $v_L=0.0075$ a.u.

As a second example, we study the transient current for di-thiol-benzene molecule (DTB) in contact with two (3,3) carbon nanotube (CNT) leads where 24 carbon atoms were used in the lead portion and total 66 atoms were included in the scattering region [see inset of Fig. 2(c)]. The structure is relaxed with the distance between the S atom and the nearest C atom equal to 2.73 a.u. and the bond length of C-C being 3.61 a.u. Figure 2 shows the transient current for different upward pulse biases. We see that for small bias $v_L=0.001$ a.u., the current drops quickly in first 50 fs and then oscillates with much slower decay rate. It is found that the oscillatory part of the transient current is dominated by $\cos(qv_L t)$ which remains valid for the transient current at other biases v_L shown in Figs. 2(b)–2(d). For instance, this gives the distance between adjacent peaks $\tau_0=152$ fs in Fig. 2(a) when $v_L=0.001$ a.u.. Different from the Al-C₄-Al structure, it takes much longer time for the system to reach the equilibrium current $I_L(\infty)=1.45 \mu\text{A}$ as shown in the inset of Fig. 2(a). From Figs. 2(a)–2(d), we conclude that the relaxation time is several ps.

Physically, this can be understood from the transmission coefficient $T(E)$. Figure 3 depicts $T(E)$ vs energy ranging

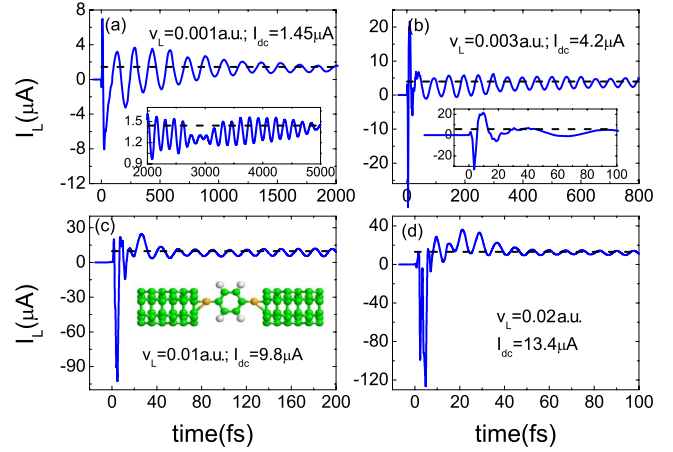


FIG. 2. (Color online) Transient current of CNT-DTB-CNT structure at different bias $v_L=0.001, 0.003, 0.01, 0.02$ a.u. The solid line shows the transient current and the dashed line is the dc current at bias $v_L-v_R=2v_L$. Inset of Fig. 2(c): schematic plot of the CNT-di-thiol benzene-CNT structure.

from the transmission threshold to Fermi energy. We have scanned 100 000 energy points in order to resolve sharp resonant peaks labeled in Fig. 3. In our calculation, 100 energy points were used for each sharp resonant peak (total 3000 energy points used) to converge the integration over ϵ , i.e., $\int d\epsilon \text{Tr}[\mathcal{J}_\alpha(\epsilon)]$ in Eq. (1). Since these sharp resonant peaks correspond to resonant states with large lifetimes, the incoming electron can dwell for a long time at these resonant states and hence the corresponding current decays much slower than the other states. If we focus on a particular resonant state with resonant energy ϵ_0 (below Fermi level) and half-width Γ_0 , then Eq. (3) gives $A_\alpha^u \sim \exp[i(\epsilon - \epsilon_0 + qv_\alpha)t - (\Gamma_0/2)t]$.¹⁴ Assuming that the sharp resonant state gives major contribution to the current (the wideband approximation), we have $A_\alpha^u \sim \exp[iqv_\alpha t - (\Gamma_0/2)t]$. Therefore the first term in Eq. (2) exhibits an oscillatory part $\exp[iqv_\alpha t - (\Gamma_0/2)t]$. Similar bias determined oscillation of transient current was also found in Ref. 20 where the oscillation frequency is determined by the bias voltage and the amplitude of oscillation is influenced by the number of resonance within the bias window.

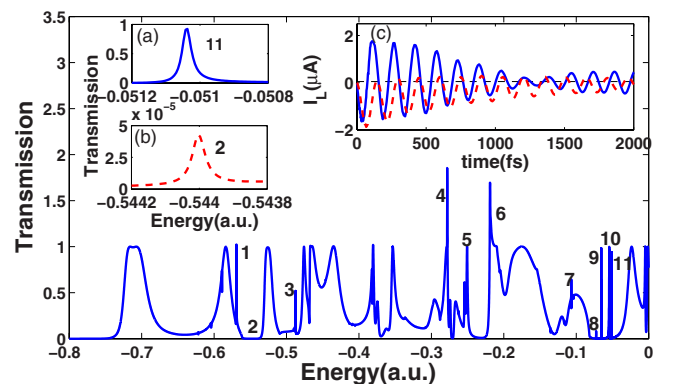


FIG. 3. (Color online) The transmission coefficient for the CNT-DTB-CNT structure. The insets are $T(E)$ vs energy at (a) peak 11 and (b) peak 2 and (c) their corresponding current.

Indeed, our numerical result confirms this analysis. It shows that these resonant peaks give major contributions to the transient current for $t > 50$ fs. In addition, we find that there is an one to one correspondence between the resonant peak at ϵ and the corresponding $\text{Tr}[\mathcal{J}_\alpha(\epsilon)]$: $\text{Tr}[\mathcal{J}_\alpha(\epsilon)]$ exhibits a huge peak whenever ϵ is near the resonance. This correspondence is important because it indicates that our ansatz has kept essential physics arising from the above analysis.

Let's examine the contribution of each resonant state to the oscillatory part of the transient current at $v_L = 0.001$ a.u. [Fig. 2(a)]. Among these resonant peaks in Fig. 3, the most contribution comes from the peak number 11 with half-width $\Gamma_{11} = 3.0 \times 10^{-5}$ a.u. as shown in the inset (a) of Fig. 3 which corresponds to a decay time $\tau_{11} = 1116$ fs from the expression $\exp(-\Gamma_{11}t)$. The second significant contribution is from the peak number 2 although the transmission coefficient of this sharp peak is very small as shown in inset (b) of Fig. 3. In inset (c) of Fig. 3, we plot the current obtained by integrating $\text{Tr}[\mathcal{J}_\alpha(\epsilon)]$ over the neighborhood of peak 2 and peak 11. It shows that the decay time is indeed characterized by τ_2 and τ_{11} . Comparing Figs. 2 and 3, we see that the contribution from the peak 2 and peak 11 to the total current is about 25% for $t < 50$ fs while for $t > 50$ fs the

contribution is more than 80%. It is the competition of these two oscillations that gives rise to the long time beat pattern of the transient current as shown in the inset of Fig. 2(a). The next dominant contribution is due to the peaks numbered 4, 6, and 9 whose contributions are one order of magnitude smaller. This indicates that one has to include all the resonant peaks for accurate results. Since different resonant peak corresponds to a different half-width Γ , one cannot choose just one Γ to characterize the system.

In summary, we have carried out first-principles investigation of time response of molecular devices. We found that the resonant states below Fermi level are crucial for time-dependent quantitative analysis. Our results indicated that the long time behavior of transient current is dominated by resonant states and the individual resonant state gives the damped oscillation with frequency equal to half of the strength of pulse bias and decay rate equal to the life time of the corresponding resonant state. Our results indicated that one has to go beyond the wide-band limit for quantitative calculations of dynamic response of molecular devices.

This work was supported by a RGC (Grant No. HKU 704308P) from the government of HKSAR.

*Corresponding author.

¹S. Kurth, G. Stefanucci, C. O. Almbladh, A. Rubio, and E. K. U. Gross, Phys. Rev. B **72**, 035308 (2005).

²Y. Zhu, J. Maciejko, T. Ji, H. Guo, and J. Wang, Phys. Rev. B **71**, 075317 (2005).

³X. Qian, J. Li, X. Lin, and S. Yip, Phys. Rev. B **73**, 035408 (2006).

⁴J. Maciejko, J. Wang, and H. Guo, Phys. Rev. B **74**, 085324 (2006).

⁵N. Sai, N. Bushong, R. Hatcher, and M. Di Ventra, Phys. Rev. B **75**, 115410 (2007).

⁶X. Zheng, F. Wang, C. Y. Yam, Y. Mo, and G. H. Chen, Phys. Rev. B **75**, 195127 (2007).

⁷G. Stefanucci, S. Kurth, A. Rubio, and E. K. U. Gross, Phys. Rev. B **77**, 075339 (2008).

⁸A. Prociuk and B. D. Dunietz, Phys. Rev. B **78**, 165112 (2008).

⁹A.-P. Jauho, N. S. Wingreen, and Y. Meir, Phys. Rev. B **50**, 5528 (1994).

¹⁰E. Runge and E. K. U. Gross, Phys. Rev. Lett. **52**, 997 (1984).

¹¹J. Taylor, H. Guo, and J. Wang, Phys. Rev. B **63**, 245407 (2001); **63**, 121104 (2001).

¹²M. Brandbyge, J. L. Mozos, P. Ordejon, J. Taylor, and K. Stokbro, Phys. Rev. B **65**, 165401 (2002).

¹³N. S. Wingreen, A. P. Jauho, and Y. Meir, Phys. Rev. B **48**, 8487

(1993).

¹⁴In *ab initio* calculation, the nonorthogonal atomic basis set can be used to calculate dc transport properties. For ac transport properties such as the transient current, however, the basis set must be orthogonalized.

¹⁵In order to use this formalism [Eq. (10)] correctly, one must be careful in the self-energy calculation where one usually adds a small imaginary part to the real energy $E \rightarrow E + i\eta$ in order to resolve the retarded or advanced self-energies. Unfortunately, this parameter η will introduce many spurious poles in the lower half plane with imaginary part of the poles less than η . This has no effect on ac current if it is calculated directly. However, if the theorem of residue is used such as Eq. (10) the transient behavior will be dominated by spurious poles. To eliminate this effect, one has to calculate the self-energy by setting $\eta = 0$.

¹⁶M. Buttiker, A. Pretre, and H. Thomas, Phys. Rev. Lett. **70**, 4114 (1993).

¹⁷B. Wang, J. Wang, and H. Guo, Phys. Rev. Lett. **82**, 398 (1999).

¹⁸We have checked that the oscillation is not due to the bound states in the scattering region by increasing the size of simulation box (Ref. 20).

¹⁹G. Stefanucci, Phys. Rev. B **75**, 195115 (2007).

²⁰P. Bokes, Phys. Chem. Chem. Phys. **11**, 4579 (2009).